https://doi.org/10.5194/egusphere-2026-4766
Preprint. Discussion started: 18 August 2026

Primary sources and secondary formation of brown carbon in urban Shanghai: Insights from bihourly measurements of brown carbon and organic tracers

Qiongqiong Wang[1,2,*], Zhongliang Huang[1], Zongjun Li[1], Shuhui Zhu[2,*] Liping Qiao[2], Min Zhou[2], Dandan Huang[2], Hongli Wang[2], Qingyan Fu[2], Kezheng Liao[3], & Jian Zhen Yu[3]

[1] Department of Atmospheric Science, School of Environmental Studies, China University of Geosciences, Wuhan, 430074, China.

[2] Laboratory of Formation and Prevention of Urban Air Pollution Complex, Ministry of Ecology and Environment, Shanghai Academy of Environmental Sciences, Shanghai 200233, China

[3] Department of Chemistry, The Hong Kong University of Science and Technology, Hong Kong 999077, China

[*]Corresponding author: Qiongqiong Wang (wangqiongqiong@cug.edu.cn) and Shuhui Zhu (Zhush@saes.sh.cn)

https://doi.org/10.5194/egusphere-2026-4766
Preprint. Discussion started: 18 August 2026

Abstract

Brown carbon (BrC) is a significant component of atmospheric carbonaceous aerosols and has important influence on climate, atmospheric chemistry, and air quality. Our knowledge about its sources and atmospheric evolution is limited due to the challenges of accurate estimation of its mass concentrations. To address this gap, we examined concurrent measurements of bihourly BrC and a suite of organic molecular tracers in urban Shanghai from March to August 2020, BrC was determined by synergistically applying the Bayesian inference (BI) model to multi-wavelength aethalometer and total carbon (TC) measurements. BrC constituted 38–40% of TC, with pronounced seasonal differences in diurnal evolution. The source apportionment analysis resolved 15 source factors and among them 7 are secondary sources, namely, secondary nitrate and sulfate formation processes, aromatic secondary organic aerosol (SOA), α-pinene SOA, β-caryophyllene SOA, isoprene SOA, oxygenated cooking OA, and secondary biomass burning. Secondary BrC accounted for 42% and 49% of total BrC in spring and summer, respectively. Seasonal contrast of the BrC contributions from primary and secondary sources were noticed. The formation mechanisms of secondary BrC were investigated by isolating events with continuous increment in secondary BrC concentrations, and the analysis suggested the diversity of oxidative pathways governing secondary BrC production. This study demonstrates the potential applicability of coupling the BI framework with online measurements of organic tracers for robust, chemically resolved BrC source apportionment. Our field observations provide the first quantitative source analysis and offer new insights into the primary sources and secondary formation of BrC in the urban atmosphere.

1. Introduction

Brown carbon (BrC) is an important yet poorly understood component of atmospheric carbonaceous aerosols, exerting profound impacts on climate, atmospheric chemistry, and air quality (Laskin et al., 2015). BrC comprises a collective mixture of light-absorbing organic substances and exhibits pronounced wavelength-dependent light absorption, contributing approximately 20% of total carbonaceous aerosol light absorption (Chung et al., 2012; Feng et al., 2013). BrC absorption can alter surface energy balance and meteorological conditions, thereby modifying ground-level $PM_{2.5}$ and O_3 concentrations (Wang et al., 2024). In addition, certain BrC chromophores can act as photosensitizers, generating various oxidants upon photon absorption (Liang et al., 2024; Lyu et al., 2026). Given these multiple and far-reaching environmental effects, a detailed understanding of BrC sources and atmospheric evolution is urgently warranted.

https://doi.org/10.5194/egusphere-2026-4766
Preprint. Discussion started: 18 August 2026

BrC can be divided into primary BrC and secondary BrC based on their emission sources. Primary BrC is predominantly emitted directly from fossil fuel combustion and biomass burning. In contrast, secondary BrC is formed in the atmosphere through diverse pathways, including gas-phase reactions, aqueous and in-cloud reactions, and heterogeneous reactions, which are driven by photochemistry, nonphotochemical reactions and droplet evaporation (Hems et al., 2021). Unlike primary BrC, which exhibits relatively stable chemical properties, secondary BrC has far more complicated formation pathways and greater variability in chemical composition, and remains considerably less understood (Li et al., 2025). Previous studies about secondary BrC have been confined to laboratory simulations of individual reaction mechanism of single compound (Kitanovski et al., 2014; Vidovic et al., 2018) or have focused on certain source type, such as biomass burning (Kuang et al., 2025), coal combustion (Ni et al., 2021), and vehicle exhaust (He et al., 2025; Lui et al., 2023). Field-based investigations, meanwhile, have largely relied on either online aerosol mass spectrometry (AMS) measurements, which offer limited molecular-level information (Qin et al., 2018), or offline filter-based analysis of molecular tracers that lack the temporal resolution to capture diel variations (Li et al., 2020b, 2026; Xiao et al., 2025; Xu et al., 2022). These methodological constraints have collectively hindered a comprehensive examination of the chemical evolution, sources, and formation mechanism of secondary BrC under real atmospheric conditions.

As BrC is an operationally defined term without a universal chemical standard, its separation from the bulk carbonaceous aerosol remains a significant challenge, yet it is essential for investigating its sources and atmospheric evolution. Early studies commonly employed a simple absorption Ångström exponent (AAE)-based approach to estimate BrC absorption in both laboratory and field measurements (Qin et al., 2018; Wang et al., 2016). Subsequent refinements, such as the BC-tracer and minimum R-squared (MRS) methods, were introduced to further separate primary from secondary BrC absorption (Hu et al., 2026; Li et al., 2020a; Wang et al., 2019a). However, these conventional approaches rely on two key assumptions: that black carbon (BC) is the sole light-absorbing component at 880 nm, and that BC is completely uncorrelated with deduced secondary BrC. Ambient aerosols are subjected to common meteorological influences, such as regional transport and boundary layer dynamics. Moreover, some secondary BrC species can be formed from precursors co-emitted with BC during combustion processes, leading to a weak but non-negligible correlation between BC and secondary BrC(Gentner et al., 2017; Jathar et al., 2013). The above approaches also lack the ability to determine BrC concentrations. To overcome these limitations, the recently developed Bayesian inference (BI) model enables the hourly determination of BrC mass concentrations by synergistically integrating total carbon (TC) measurements with multi-wavelength aethalometer data (Liao et al., 2024). This advancement provides a unique opportunity to delve

https://doi.org/10.5194/egusphere-2026-4766
Preprint. Discussion started: 18 August 2026

more deeply into the primary and secondary BrC. Complementarily, organic-tracer based source apportionment using positive matrix factorization (PMF) model has been widely employed to distinguish secondary organic carbon (SOC) from primary organic carbon (POC)(Wang et al., 2017, 2019b). Notably, when combined with high-time-resolution measurements of a comprehensive suite of organic molecular tracers, this method can resolve contributions from specific emission sources-beyond bulk organic aerosol factors-and elucidate their diel variations and formation processes (Li et al., 2020a; Zhu et al., 2021). Its applicability has recently been extended to the separation of secondary versus primary organic nitrogen as well (Yu et al., 2025). By integrating high-time-resolution organic tracer data with BI-derived BrC mass concentrations, it is possible to separate secondary BrC and investigate its formation mechanisms and driven factors under real atmospheric conditions.

In this study, we quantified hourly BrC concentrations in urban Shanghai from March to August 2020 using the BI method, based on online measurements of multi-wavelength light absorption and TC. Concurrently, a comprehensive suite of bihourly organic molecular tracers-representative of distinct primary emission sources and secondary formation processes-were measured alongside major aerosol chemical components and elemental tracers. These high time resolution measurement data enabled us to quantitatively apportion BrC sources and examine its dynamic evolution in the atmosphere, using an organic-tracer based source apportionment model. Furthermore, we investigated the sources and chemical evolution of secondary BrC to complement our current limited knowledge about its formation and atmospheric evolution.

2. Methodology

2.1 Sampling site and measurement period

The field measurements were conducted at the Shanghai Academy of Environmental Sciences (SAES, 31.10°N, 121.25°E), located in the Xuhui district of urban Shanghai, China. The sampling site can be regarded as a receptor site influenced by mixed sources emissions from both local and regional contributions. Measurements were carried out from 1 March to 31 August 2020, encompassing the spring (March-May) and summer (June-August) seasons.

2.2 Online attenuation measurement and BrC mass concentration estimation using the BI modeling

Online multi-wavelength light absorption data were measured using an Aethalometer (AE30, Magee Scientific, U.S.A.). Raw Aethalometer measurements are subject to several artifacts, including the filter matrix effect (multiple scattering), the loading effect (shadowing) and the scattering effect. In this study, we applied the Weingartner correction method (Weingartner et al., 2003) to correct the filter-loading effect associated with particle

https://doi.org/10.5194/egusphere-2026-4766
Preprint. Discussion started: 18 August 2026

accumulation on the filter, using Eq1-2. The aerosol light absorption coefficients in ambient air (b_{abs}) were subsequently calculated by correcting the multiple-scattering effect caused by the filter matrix, following Eq3.

$$eBC_{corrected}=\frac{eBC_{raw}}{R(ATN)} \quad (1)$$

$$R(ATN)=\left(\frac{1}{f}\text{-}1\right)\times\frac{\ln(ATN)-\ln(10)}{\ln(50)-\ln(10)}+1 \quad (2)$$

$$b_{abs}=\frac{eBC_{corrected}\times\sigma_{ATN}}{C} \quad (3)$$

Where $eBC_{corrected}$ denotes the corrected equivalent BC mass concentration, and eBC_{raw} represents the raw equivalent BC concentrations prior to correction. ATN is the filter attenuation, and f is an empirical compensation parameter for the filter loading effect. The parameter f was determined using the Aethalometer Data Processor (ADP) developed on the Igor Pro platform (Wu et al., 2018). Different f values were evaluated by examining the continuity and smoothness of the corrected time series across filter change points. The optimal continuity for the absorption coefficients at all wavelengths was achieved with f = 1.15, which was therefore adopted in this study. σ_{ATN} is the mass absorption cross section of BC. C is the multiple-scattering parameter, which depends on the filter material and the mixing state of the particles. Following previous studies, a value of C=3.5 was adopted herein (Wu et al., 2024a).

After obtaining the corrected b_{abs} data, hour-by-hour BrC mass concentrations were subsequently estimated via the BI method, following Eq4-5. The BI model inputs included the corrected seven-wavelength light absorption coefficients (i.e., b_{370}、b_{470}、b_{520}、b_{590}、b_{660}、b_{880} and b_{950}) and hourly TC concentrations, which were measured by an RT-4 carbon analyzer (Sunset Laboratory Inc., U.S.A.).

$$TC = BC + BrC + WtC \quad (4)$$

$$b_{\lambda_i} = MAE_{\lambda_i}^{BC} \times BC + \left(K^{BrC} \times \lambda_i^{-AAE^{BrC}}\right) \times BrC, i = 1,2,3 \ldots,7 \quad (5)$$

Where TC, BC, BrC and WtC are the concentrations of TC and its three carbon components. $MAE_{\lambda_i}^{BC}$ is the mass absorption efficiency of BC at wavelength λ_i. K^{BrC} is a sample-dependent constant, and AAE^{BrC} describes the wavelength dependence of light absorption for BrC. We adopted the likelihood function and prior distributions parameterization established in previous studies (Li et al., 2026; Liao et al., 2024). Detailed principles of the BI model and its parameter settings are described in Liao et al. (2024).

2.3 Online measurements of organic tracers and other supportive data

https://doi.org/10.5194/egusphere-2026-4766
Preprint. Discussion started: 18 August 2026

Bihourly organic markers were measured using an Aerodyne TAG coupled with a GC-MS system (Agilent GC 7890B/MSD 5977B), and detailed instrumental specifications and data quality assurance procedures are described in Wang et al. (2026) and Zhu et al. (2025) In this study, 1-h ambient samples were collected and analyzed at every even hour. Due to instrument maintenance, data were unavailable during 21/5-16/6 and 29/7-14/8. A comprehensive suite of organic tracers was measured, including saccharides, nitroaromatic compounds (NACs), polycyclic aromatic hydrocarbons (PAHs), fatty acids, hopanes and secondary organic aerosol (SOA) tracers. Polar organic compounds were derivatized to their trimethylsilyl derivatives under a helium stream saturated with the derivatization agent N-methyl-N-(trimethylsilyl) trifluoroacetamide (MSTFA), whereas non-polar organic compounds were analyzed directly after thermal desorption by GC-MS.

Complementary PM chemical speciation measurements included hourly $PM_{2.5}$ mass concentrations measured using a beta attenuation particulate monitor (FH62-C14, Thermo Fisher, U.S.A.), water-soluble inorganic ions by MARGA (Metrohm, Switzerland), and trace elements by a Xact 625 X-ray fluorescence multi-metal analyzer (Cooper Environmental, U.S.A.). In addition, gaseous pollutants (CO, NO_x, SO_2, and O_3) and meteorological parameters (wind direction, wind speed, temperature, and relative humidity) were concurrently monitored.

2.3. Organic-tracer based source apportionment for BrC by PMF

In this study, the EPA PMF 5.0 model was employed to apportion the sources of BrC. Previous studies have demonstrated that incorporating source-specific organic tracers enables more accurate source estimation of $PM_{2.5}$ and OC (Wang et al., 2017, 2019b). Unlike conventional PMF applications, our analysis specifically targeted the source apportionment for BrC mass concentrations. We incorporated a comprehensive organic tracer data with the effort to resolve more detailed sources for BrC, especially secondary BrC. The input species for the PMF model included three BI-derived carbonaceous components (BC, BrC and WtC), three water-soluble inorganic species (SO_4^{2-},NO_3^-, and NH_4^+), ten elements (K, Ca, Cr, Mn, Fe, Ni, Zn, Se, Ba, and Pb), and ten organic molecular tracers measured by TAG (fatty acids, hopanes, PAHs, NACs, saccharides, azelaic acid, aromatic SOA tracers, isoprene SOA tracers, α-pinene SOA tracers, and β-caryophyllinic acid). A complete list of input species is provided in Table S1.

To evaluate the stability of the PMF solution, bootstrapping (BS) and displacement (DISP) analysis were performed. A BS mapping frequency exceeding 80% (with a correlation coefficient $R \geq 0.6$ between the BS factors and the base-run factors) was considered indicative of stable factor assignment. The DISP results were deemed acceptable when no significant decrease in the scaled residual Q (i.e., $\%dQ < 1\%$) and no factor swapping were observed.

https://doi.org/10.5194/egusphere-2026-4766
Preprint. Discussion started: 18 August 2026

3. Results and discussion

3.1 Abundance and variations of BrC

The temporal variations in aerosol components, organic tracers, and meteorological conditions over the entire field measurements are presented in Figure 1, with seasonal and period-average concentrations summarized in Table S1. Throughout the study, $PM_{2.5}$ mass concentrations exhibited a wide range (3.6 to 111.1 μg/m^3), with higher levels observed in spring (33.0±20.9 μg/m^3) compared to summer (26.0±15.3 μg/m^3). TC concentrations ranged from 0.89-19.9 μg/m^3, averaging 4.95±2.71 μg/m^3 in spring and 4.65±2.65 μg/m^3 in summer, contributing 12% and 16% to $PM_{2.5}$ mass, respectively. BrC concentrations ranged from 0.25-13.62 μg/m^3, with average values of 1.47±1.23 μg/m^3 in spring and 1.63±1.17 μg/m^3 in summer. BrC contributed 38% and 39% to TC mass and 4% and 6% to $PM_{2.5}$ mass in spring and summer, respectively. TAG-measured total organics were higher in summer (314.0±216.5 ng/m^3) than in spring (216.1± 141.1 ng/m^3). The predominant species transitioned from fatty acids (42%) and saccharides (36%) in spring to isoprene SOA tracers (36%) in summer, alongside fatty acids (26%) and saccharides (23%). The naming and grouping of the organic tracers are shown in Table S2.

The monthly diurnal variations of BrC are presented in Figure 2. Generally, the relative abundance of BrC in total TC remained relatively stable throughout the study period, contributing 38-40% to TC mass. In spring, obvious enhanced BrC concentrations was observed from March to May, yet no apparent diurnal pattern was observed. In contrast, during summer (June–August), BrC concentrations were comparable across months but exhibited distinctly higher daytime levels, with a bimodal distribution characterized by a noontime peak (11:00–15:00) and an evening peak (18:00–20:00). The noontime peak was most pronounced in August, suggesting enhanced daytime formation. These contrasting seasonal behaviors indicated that BrC in spring and summer are governed by different formation pathways and emission sources. Accordingly, further investigations into the chemical composition, sources, and atmospheric evolution of BrC—particularly its secondary fraction—are warranted.

https://doi.org/10.5194/egusphere-2026-4766
Preprint. Discussion started: 18 August 2026

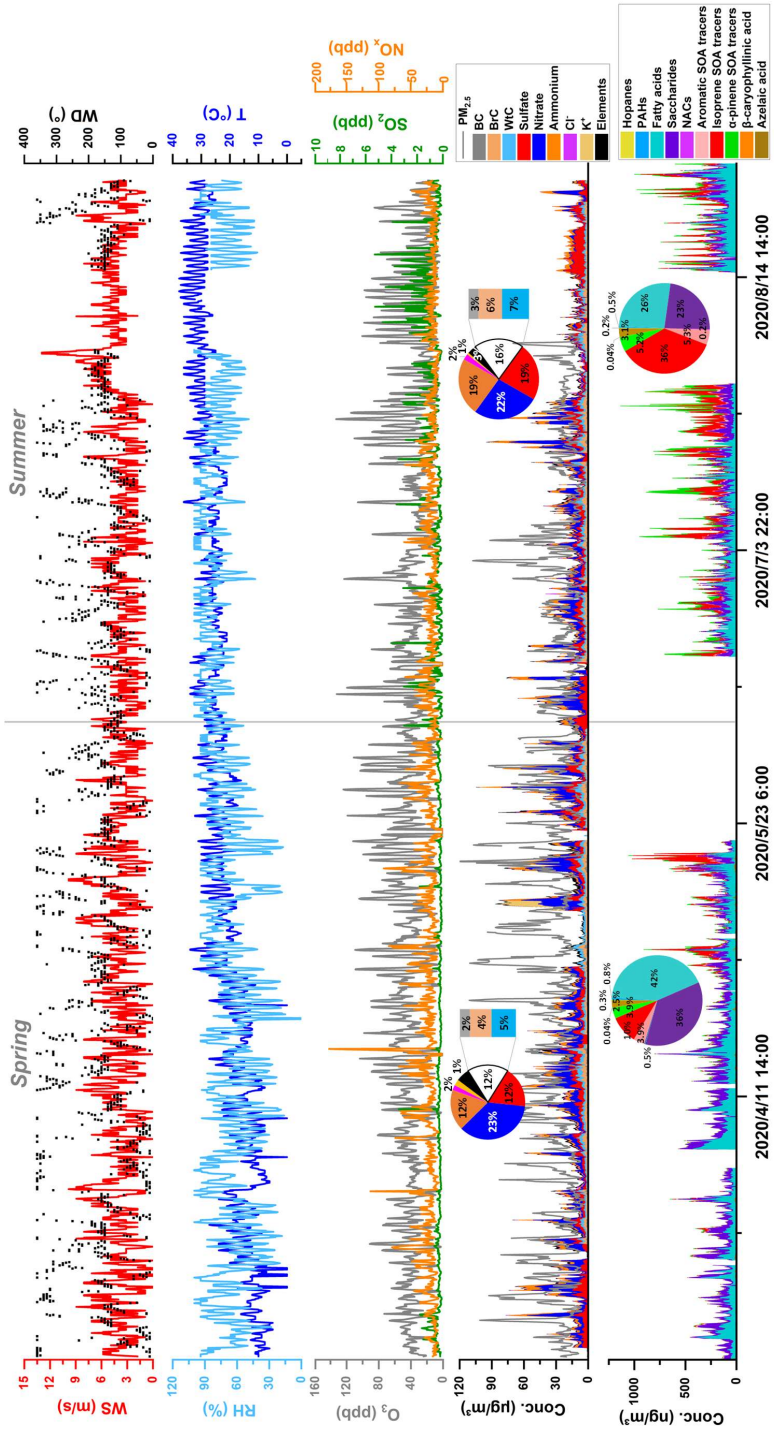

Figure 1. Temporal variations of $PM_{2.5}$ bulk components, carbonaceous aerosols, organic tracers, gaseous pollutants (SO_2, NO_x, and O_3), and meteorological parameters (temperature-T, relative humidity-RH, wind speed-WS, and wind direction-WD) during the campaign period in Shanghai.

https://doi.org/10.5194/egusphere-2026-4766
Preprint. Discussion started: 18 August 2026

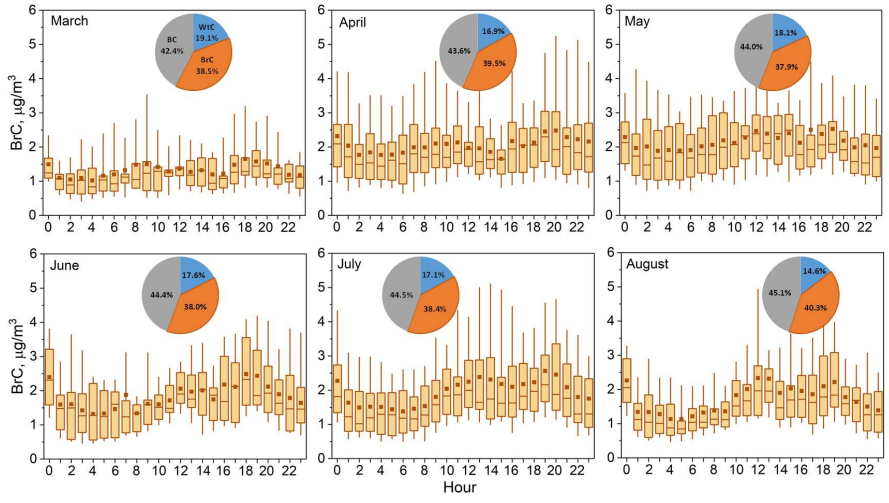

Figure 2. Monthly diurnal variations of BrC during the study period from 1/3/2020-31/8/2020 in Shanghai (squares and solid lines correspond to mean and median values, respectively; box indicates the 25th and 75th percentiles, and whiskers are the 10th and 90th percentiles). The insert pie chart shows the fraction of the three carbon components (i.e., BC, BrC and WtC).

3.2. Source apportionment of BrC by PMF with organic and elemental tracers

The sources of BrC were evaluated using the PMF model, taking advantage of the comprehensive chemical speciation dataset, especially the high-time-resolution measurements of source-specific organic tracers and BI-derived BrC concentrations. To accentuate seasonal differences, spring and summer data were input separately into the PMF model. Unlike previous source apportionment studies in this region, which focused on bulk $PM_{2.5}$ or OC, our analysis specifically targets BrC mass. The inclusion of a suite of bihourly source-specific organic and elemental tracers enabled us to resolve previously unidentified sources and capture rapid fluctuations in source activities and atmospheric processes. This facilitated robust diurnal pattern analysis of source contributions—a temporal resolution unattainable in earlier work and critical for deriving accurate source estimates(Wang et al., 2018). Five to eighteen factors were initially tested, and a fifteen-factor PMF solution was selected for both seasonal datasets. The error estimation results of the PMF runs (summarized in Tables S3&S4) indicated that the selected PMF runs passed the BS and DISP tests, confirming robust solutions. The PMF-predicted BrC mass agreed well with measured values, with slope of 0.82 and R_p of 0.91 (Figure S1). The factor profiles of the fifteen-factor solutions are shown in Figure 3 and temporal trends and diurnal variations of individual factor contributions are presented in Figures S2-S3, while Figure 4 highlights the diurnal variations of each factor's percentage contributions to BrC.

Factor identification was based on established organic and elemental tracers and is generally consistent with previous studies in this region (Wang et al., 2018; Zhu et al., 2021). Briefly, the secondary nitrate and sulfate formation process factor was identified by high loadings of sulfate,

https://doi.org/10.5194/egusphere-2026-4766
Preprint. Discussion started: 18 August 2026

ammonium and nitrate (Figure 3). BrC associated with this factor reflects formation pathways similar to those of secondary inorganic aerosols. This factor exhibited higher percentage contributions during nighttime hours, with more pronounced contributions in spring (Figure 4). Among SOA factors, we resolved aromatic SOA factor, α-pinene SOA, isoprene SOA and β-caryphyllene SOA based on their respective tracers, which trace back to specific volatile organic compound (VOC) precursors. Distinct diurnal patterns were observed for these SOA factors. Aromatic SOA showed comparable seasonal contributions with higher daytime values in both seasons. α-pinene SOA peaked at late afternoon hours (16:00-20:00), particularly in summer. β-caryphyllene SOA contributed more in spring overall, but with higher daytime contributions in summer. Isoprene SOA was substantially enhanced in summer, with nighttime dominance. The oxygenated cooking OA factor was identified by azelaic acid, which was the main oxidation products of unsaturated fatty acids such as oleic acid (Wang and Yu, 2021). This factor showed clear noontime and dinner-time peaks, with higher contributions in summer (Figure 4). During dinner hours (20:00-22:00), average contributions reached 15-20% of total BrC. Secondary biomass burning was identified by NACs, and it showed comparable seasonal contributions with slightly higher daytime values. Biomass burning was identified by saccharides and it contributed more during nighttime hours, with similar magnitude across seasons. The cooking emission factor was identified by fatty acids, and this factor showed higher contributions in spring, with distinct noontime and dinner times peaks. Vehicle exhaust factor was identified by high loadings of hopanes, while tire wear was characterized by high loadings of Mn and Fe, typical non-exhaust emission tracers (Wang et al., 2018). Both factors correlated well with NO_x (Figure S4), and displayed clear morning rush-hour peaks (Figure 4), confirming their traffic origin. The two factors both showed higher contributions in spring. Re-suspended road dust was identified by Ca and Ba and it showed bimodal distributions with higher daytime contributions, indicating the resuspension of road dust caused by passing vehicles (Wang et al., 2022). This factor showed comparable seasonal contributions. Coal combustion, identified by PAHs, also showed higher contributions in spring. Power plant combustion, identified by Cr, Zn and Se, exhibited higher contributions in summer. Residual oil combustion was identified by Ni, with higher contributions in spring.

https://doi.org/10.5194/egusphere-2026-4766
Preprint. Discussion started: 18 August 2026

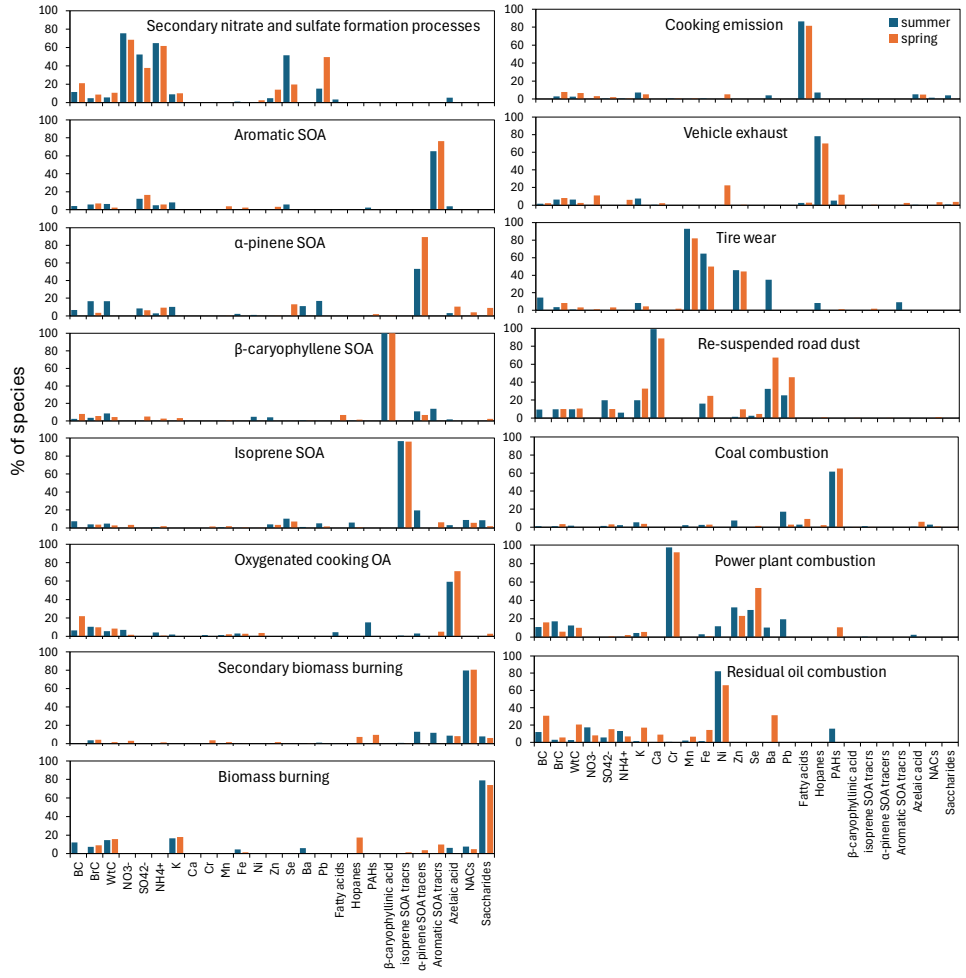

275

276 **Figure 3.** (a) Source profiles (percentage of species) of individual factors resolved by organic tracer-
277 based PMF model using measurement data in spring (March-May) and summer (June-August).

https://doi.org/10.5194/egusphere-2026-4766
Preprint. Discussion started: 18 August 2026

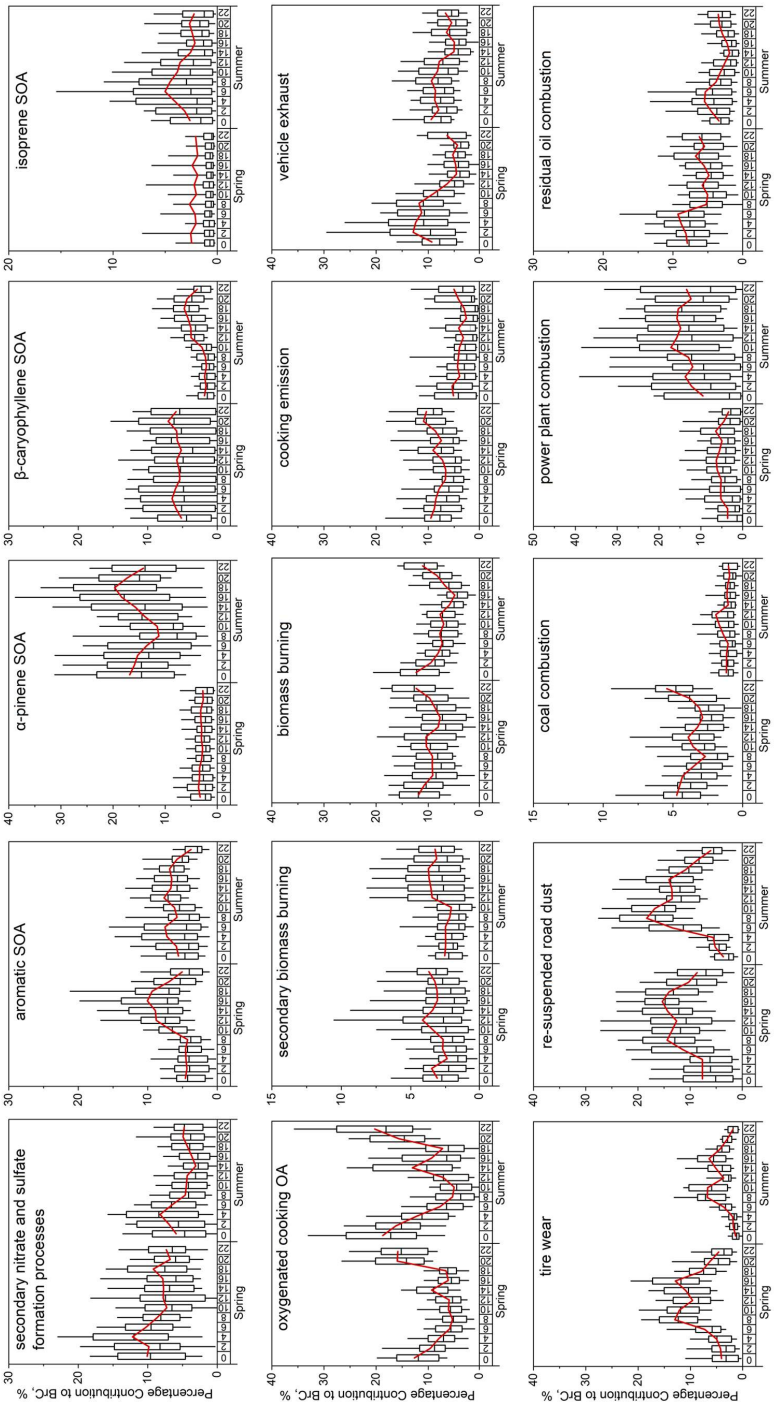

Figure 4. Diurnal variation of individual factor contributions to BrC from PMF results (25th and 75th percentile boxes, 10th and 90th percentile whiskers; the dashed line is the median value, and the solid red line is the mean value).

https://doi.org/10.5194/egusphere-2026-4766
Preprint. Discussion started: 18 August 2026

Figure 5a&b shows the seasonal and diurnal average of source contributions to BrC. Briefly, BrC mass were dispersed into different sources, reflecting its diverse emission sources in the complex urban atmosphere. BrC derived from the secondary sources are regarded as secondary BrC, namely, secondary nitrate and sulfate formation processes, aromatic SOA, α-pinene SOA, β-caryophyllene SOA, isoprene SOA, oxygenated cooking SOA, and secondary biomass burning. Overall, 58% (0.92 μg/m^3) and 51% (0.89 μg/m^3) of the BrC mass was attributed to primary emissions. Among the primary sources, re-suspended road dust, biomass burning and vehicle exhaust were the major sources in spring, contributing to 10%, 9%, and 8% of BrC, respectively. While in summer, power plant combustion, re-suspended road dust and biomass burning were the major contributors, with contributions of 17%, 10%, and 7% of BrC, respectively. Besides well-documented contributions of biomass burning and vehicle exhaust to BrC, we identified significant portion of BrC from re-suspended road dust, suggesting the importance of the non-exhaust emission to BrC. Figure 5c shows the variations of the source contributions with increasing BrC mass. Among the primary sources, power plant combustion showed both increased mass and enhanced percentage contribution with increasing BrC mass, especially in summer, suggesting the importance of coal combustion in power plants as major primary sources.

Secondary BrC accounted for significant proportions of the total BrC in both seasons, with contributions of 42% (0.67 μg/m^3) and 49% (0.85 μg/m^3) in spring and summer, respectively (Figure 5a). Seasonal contrast of the composition of the secondary BrC was noticed between spring and summer. In spring, the major source contributors to secondary BrC were oxygenated cooking OA and secondary sulfate and nitrate formation processes, contributing to 9.6% and 8.8% of BrC, respectively. In summer, the main contributors were α-pinene SOA and oxygenated cooking OA, contributing to 16.5% and 10.4% of BrC, respectively. Decrease of the total secondary BrC was noticed in the nighttime to early morning hours during 20:00-08:00, while the total secondary BrC gradually increased from 08:00-14:00, especially in summer (Figure 5b). Enhanced secondary proportion was observed with increased BrC mass, suggesting the increasing significance of secondary production of BrC (Figure 5c). Among the seven secondary sources, isoprene SOA and secondary biomass burning exhibited both increased mass and enhanced percentage contribution with increasing BrC mass, suggesting their important roles in secondary BrC formation.

https://doi.org/10.5194/egusphere-2026-4766
Preprint. Discussion started: 18 August 2026

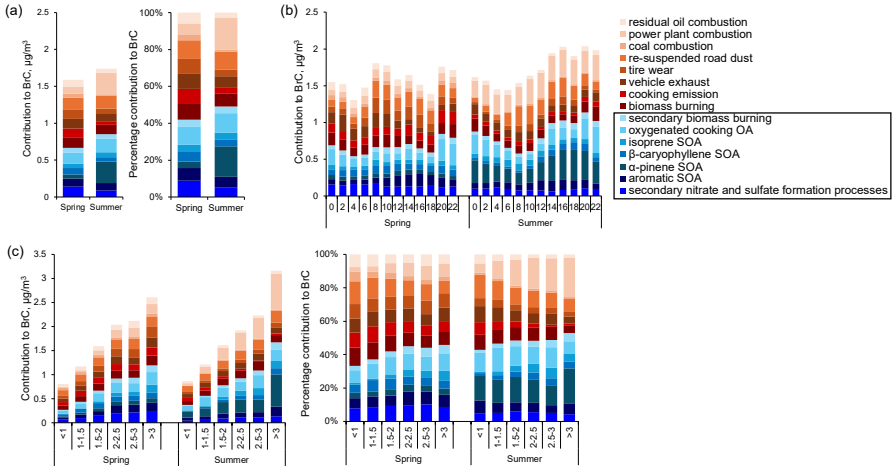

312

313 **Figure 5.** (a) Seasonal average of mass and percentage contributions of individual source
314 factors to BrC; (b) diurnal variations of the source contributions to BrC; (c) average mass and
315 percentage contributions of individual source factors to BrC grouped by different BrC mass
316 concentrations.

317

318 **3.3. Factors driven the increment of secondary BrC**

319 To further investigate the formation mechanisms of secondary BrC under varying urban
320 atmosphere, we focus on the cases where secondary BrC concentrations showed continuous
321 increment for at least for 6 consecutive hours and remained above the period-mean abundance.
322 Overall, we extracted a total of 26 such events and Figure S5 shows their temporal distributions.
323 Summer accounted for the majority of these events (17 out of 26), indicating more frequent
324 secondary BrC formation during the warmer season. To distinguish between local formation
325 and regional transport, we classified events based on wind speed, following previous studies
326 (Yu et al., 2025; Zhou et al., 2022). Wind speed exceeding 3 m/s were taken to indicate the
327 impact from local air masses, thereby representing local secondary BrC formation. Under this
328 criterion, a total of nine local formation events were observed, suggesting that regional
329 transport was the dominant driver of secondary BrC enhancement, particularly in summer. In
330 this study, we mainly focus on these nine local formation events in the following analysis. Based
331 on their characteristic contributing sources, the nine events were further categorized into six
332 distinct types and Table S5 summarizes the occurrence time and the associated gas pollutants
333 and meteorological conditions for each of these events.

334 Figure 6 plots the source contributions to secondary BrC during the six types of local
335 formation events. Type 1, observed from midnight to early morning in spring, exhibited a total
336 BrC increment of 0.39 μg/m^3. This increase was predominantly driven by secondary biomass

https://doi.org/10.5194/egusphere-2026-4766
Preprint. Discussion started: 18 August 2026

burning, which contributed 0.27 μg/m^3, accounting for 69% of the total secondary BrC increment. The elevated BrC can be attributed to enhanced formation of NACs, such as 4-nitrocatechol, through nitration of phenolic VOCs emitted by biomass burning via gas-phase or aqueous-phase pathways (Mayorga et al., 2021). Notably, the main sources of secondary BrC in this event is secondary nitrate and sulfate formation processes, which shared NO_x, a common precursor with NACs formation, suggesting a concurrent formation regime. Type 2 featured secondary nitrate and sulfate formation processes as the dominant driver of secondary BrC increment, accounting for 82% of the total increment (0.33 μg/m^3). This event also occurred from midnight to early morning, underscoring the importance of nocturnal nitrate formation processes (Zhou et al., 2022). This fraction of secondary BrC likely reflects the formation of organic nitrates, which are recognized as important BrC components (Wu et al., 2024b). Typical formation pathways of organic nitrates include NO_3-initiated oxidation of alkenes, which proceeds efficiently during nighttime hours (Yu et al., 2019). Type 3 occurred from afternoon to nighttime with the largest increment during dinner hours (20:00-22:00) and it showed a total secondary BrC increment of 0.59 μg/m^3. Oxygenated cooking OA was the predominant contributor, contributing to 108% of the total increment. This factor also dominated the overall secondary BrC composition during this event. Importance of cooking emissions to OC at this site has been reported in previous studies (Wang and Yu, 2021), the results in this study suggest that oxygenated cooking OA can contribute significantly to BrC, possibly due to nitration reactions of cooking-emitted unsaturated fatty acids, forming nitrogen-containing organics (Hung et al., 2005). Type 4 occurred in the morning and showed a moderate BrC increment (0.22 μg/m^3). This event was featured by aromatic SOA as the driving factor to secondary BrC increment, contributing to 127% of the net increase. The ambient conditions during this event showed high concentrations of NO_x, high RH, but notably low ozone concentrations (Table S5). The results suggested the importance NO_x-initiated oxidation of aromatic VOCs, producing nitrogen-containing organics which are known chromophores contributing to BrC. Type 5 occurred in daytime and persisted for 8 hours and was dominated by isoprene SOA, which contributed 61% of the total BrC increment. The largest increment occurred around noontime (12:00-14:00), coinciding with peak solar radiation. This event was characterized by high temperatures and elevated ozone concentrations, underscoring the dominant role of photochemical formation in producing isoprene SOA. Type 6 events, totaling four, occurred in summer. Figure 6 shows a representative case and the remaining three presented in Figure S6. These events occurred during daytime under elevated ozone levels and exhibited the largest secondary BrC increment (2.27 μg/m^3). α-pinene SOA was the predominant contributor, accounting for 60% of the total BrC increase. The maximum increment was recorded in the afternoon (14:00-16:00) with the highest ozone concentrations, indicating enhanced photochemical formation of α-pinene SOA under strong oxidative conditions.

https://doi.org/10.5194/egusphere-2026-4766
Preprint. Discussion started: 18 August 2026

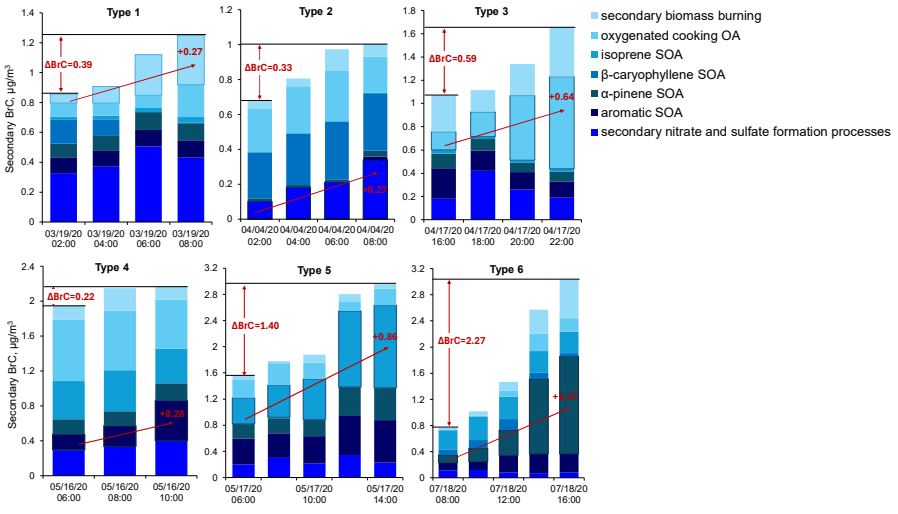

Figure 6. Six types of secondary BrC increment events with different dominant formation pathways observed across the field measurements. Type 1 was driven by secondary biomass burning, type 2 by secondary nitrate and sulfate formation processes, type 3 by oxygenated cooking OA, type 4 by aromatic SOA, type 5 by isoprene SOA and type 6 by α-pinene SOA.

4 Conclusions

Accurate estimation of BrC mass from the carbonaceous aerosols remains a significant challenge, hindering robust evaluation of its climatic and air quality impacts. In this study, we quantified hourly BrC mass concentrations in urban Shanghai from March to August 2020 by synergistically applying the BI model to multi-wavelength aethalometer and TC measurements, overcoming the methodological limitations inherent in conventional optical-based separation approaches. The BI-derived BrC accounted for 38-40% of total TC across the study period, with distinct diurnal patterns observed between spring and summer months, pointing to seasonally varying sources and formation pathways. Taking advantage of a comprehensive suite of concurrently measured bihourly organic and elemental tracers, we apportioned BrC sources and disentangled primary versus secondary BrC using an organic-tracer-based PMF model. A total of 15 factors were resolved, including 7 secondary sources, each exhibiting characteristic diurnal profiles. Overall, secondary BrC contributed 42% and 49% of total BrC in spring and summer, respectively. Seasonal contrast of the source contributions to secondary BrC was observed, with dominant contributors of oxygenated cooking OA and secondary sulfate and nitrate formation processes in spring and α-pinene SOA and oxygenated cooking OA in summer. Case studies of secondary BrC increment events further revealed the

https://doi.org/10.5194/egusphere-2026-4766
Preprint. Discussion started: 18 August 2026

involvement of diverse precursors and chemical processes, underscoring the complexity of secondary BrC formation and evolution in the urban atmosphere.

This study demonstrates the powerful applicability of integrating the BI model with organic-tracer-based PMF analysis for source apportionment of atmospheric BrC. The high-time-resolution quantification of secondary BrC from multiple sources provides unprecedented insight into its dynamic formation mechanisms under ambient conditions, complementing laboratory-based mechanistic studies. Our findings offer a scientific basis for developing targeted mitigation strategies aimed at reducing BrC emissions and improving air quality in urban environments.

https://doi.org/10.5194/egusphere-2026-4766
Preprint. Discussion started: 18 August 2026

Data availability

Data used in this study are available upon request from the corresponding author.

Author contributions

QW: conceptualization, formal analysis, writing-original draft; ZH and ZL: data curation; SZ: measurements of the organic tracers, writing-review and editing. LQ, MZ, DH, HW, QF and KL: data curation, and YJZ: writing-review and editing.

Competing interests

The contact author has declared that none of the authors has any competing interests.

Financial support

This research has been supported by National Natural Science Foundation of China (42305107 and 42307155), the "CUG Scholar" Scientific Research Funds at China University of Geosciences (Wuhan) (Project No. 2022115), and Hong Kong Research Grants Council (T24-614/25N).

References

Chung, C. E., Ramanathan, V., and Decremer, D.: Observationally constrained estimates of carbonaceous aerosol radiative forcing, Proc. Natl. Acad. Sci. U. S. A., 109, 11624–11629, https://doi.org/10.1073/pnas.1203707109, 2012.

Feng, Y., Ramanathan, V., and Kotamarthi, V. R.: Brown carbon: a significant atmospheric absorber of solar radiation?, Atmos. Chem. Phys., 13, 8607–8621, https://doi.org/10.5194/acp-13-8607-2013, 2013.

Gentner, D. R., Jathar, S. H., Gordon, T. D., Bahreini, R., Day, D. A., Haddad, I. El, Hayes, P. L., Pieber, S. M., Platt, S. M., Gouw, J. De, Goldstein, A. H., Harley, R. A., Jimenez, J. L., Pre, A. S. H., and Robinson, A. L.: Review of Urban Secondary Organic Aerosol Formation from Gasoline and Diesel Motor Vehicle Emissions, Environ. Sci. Technol., 51, 1074−1093, https://doi.org/10.1021/acs.est.6b04509, 2017.

He, X., Zheng, X., Jiang, B., Cao, X., Chen, T., Guo, S., Li, Z., Ding, Y., Zhang, S., Cheng, Y., Jiang, J., Wang, S., and Wu, Y.: Correction to: Significant N-containing brown carbon emission from heavy-duty diesel vehicles revealed by the molecular and chromophore analysis using ultra-high resolution mass spectrometry (npj Climate and Atmospheric Science, (2025), 8, 1, (200), 10.1038/s41612-025-01034-8), npj Clim. Atmos. Sci., 8, https://doi.org/10.1038/s41612-025-01129-2, 2025.

Hems, R. F., Schnitzler, E. G., Liu-Kang, C., Cappa, C. D., and Abbatt, J. P. D.: Aging of Atmospheric Brown Carbon Aerosol, ACS Earth Sp. Chem., 5, 722–748, 2021.

Hu, K., Liao, H., Liu, D., Wang, Y., Liu, Q., Liu, Z., Bi, K., Zhao, D., Li, S., Wu, Y., Tian, P.,

https://doi.org/10.5194/egusphere-2026-4766
Preprint. Discussion started: 18 August 2026

Wang, F., Hu, B., Jiang, X., and Zhao, S.: Influence of Secondary Brown Carbon Aerosol Lifetime on Radiative Properties, Geophys. Res. Lett., 53, e2026GL122385, https://doi.org/10.1029/2026GL122385, 2026.

Hung, H., Katrib, Y., and Martin, S. T.: Products and Mechanisms of the Reaction of Oleic Acid with Ozone and Nitrate Radical, J. Phys. Chem. A, 109, 4517–4530, 2005.

Jathar, S. H., Miracolo, M. A., Tkacik, D. S., Donahue, N. M., Adams, P. J., and Robinson, A. L.: Secondary Organic Aerosol Formation from Photo-Oxidation of Unburned Fuel: Experimental Results and Implications for Aerosol Formation from Combustion Emissions, Environ. Sci. Technol., 47, 12886−12893, 2013.

Kitanovski, Z., Cusak, A., Grgic, I., and Claeys, M.: Chemical characterization of the main products formed through aqueous-phase photonitration of guaiacol, Atmos. Meas. Tech., 7, 2457–2470, https://doi.org/10.5194/amt-7-2457-2014, 2014.

Kuang, Y., Luo, B., Huang, S., Liu, J., Hu, W., Peng, Y., and Chen, D.: Formation of highly absorptive secondary brown carbon through nighttime multiphase chemistry of biomass burning emissions, Atmos. Chem. Phys., 25, 3737–3752, 2025.

Laskin, A., Laskin, J., and Nizkorodov, S. A.: Chemistry of Atmospheric Brown Carbon, Chem. Rev., 115, 4335–4382, https://doi.org/10.1021/cr5006167, 2015.

Li, R., Wang, Q., He, X., Zhu, S., Zhang, K., Duan, Y., Fu, Q., and Qiao, L.: Source apportionment of PM 2.5 in Shanghai based on hourly organic molecular markers and other source tracers, Atmos. Chem. Phys., 5, 12047–12061, 2020a.

Li, X., Yang, Y., Liu, S., Zhao, Q., Wang, G., and Wang, Y.: Light absorption properties of brown carbon (BrC) in autumn and winter in Beijing: Composition, formation and contribution of nitrated aromatic compounds, Atmos. Environ., 223, 117289, https://doi.org/10.1016/j.atmosenv.2020.117289, 2020b.

Li, Y., Fu, T.-M., Yu, J. Z., Zhang, A., Yu, X., Yu, J., Zhu, L., Shen, H., Wang, C., Yang, X., Tao, S., Chen, Q., Li, Y., Li, L., Che, H., and Heald, C. L.: Nitrogen dominates global atmospheric organic aerosol absorption, Science (80-.)., 387, 989–995, https://doi.org/10.1126/science.adr4473, 2025.

Li, Z., Wang, Q., Zhao, Y., Huang, Z., and Liao, K.: Seasonal variability and sources of brown carbon in Wuhan : Insights from Bayesian modeling and organic tracers-based source apportionment, Atmos. Res., 333, 108736, https://doi.org/10.1016/j.atmosres.2025.108736, 2026.

Liang, Z., Li, Y., Go, B. R., and Chan, C. K.: Complexities of Photosensitization in Atmospheric Particles, ACS ES&T Air, 1, 1333–1351, https://doi.org/10.1021/acsestair.4c00112, 2024.

Liao, K., Cheng, Y. Y., Yea, S. S., Chen, L. A., Seinfeld, J. H., and Yu, J. Z.: New Analytical Paradigm to Determine Concentration of Brown Carbon and Its Sample-by-Sample Mass Absorption Efficiency, Environ. Sci. Technol., 58, 17386–17395, https://doi.org/10.1021/acs.est.4c06831, 2024.

Lui, K. H., Lau, Y., Poon, H. Y., Organ, B., Chan, M., Guo, H., Sai, S., Ho, S. S. H., and Ho, K. F.: Characterization of chemical components of fresh and aged aerosol from vehicle exhaust emissions in Hong Kong, Chemosphere, 333, 138940, https://doi.org/10.1016/j.chemosphere.2023.138940, 2023.

Lyu, Y., Li, Y., Ma, R., Zhou, T., Borduas-dedekind, N., and Nah, T.: Connecting Brown Carbon Composition and Physicochemical Properties of Aqueous Urban PM2.5 to their Photosensitized Production of Singlet Oxygen and Organic Triplet Excited States, Environ.

https://doi.org/10.5194/egusphere-2026-4766
Preprint. Discussion started: 18 August 2026

Sci. Technol., 60, 6442–6453, https://doi.org/10.1021/acs.est.5c15686, 2026.

Mayorga, R. J., Zhao, Z., and Zhang, H.: Formation of secondary organic aerosol from nitrate radical oxidation of phenolic VOCs: Implications for nitration mechanisms and brown carbon formation, Atmos. Environ., 244, 117910, https://doi.org/10.1016/j.atmosenv.2020.117910, 2021.

Ni, H., Huang, R., Pieber, S. M., Corbin, J. C., Stefenelli, G., Pospisilova, V., Klein, F., Gysel-beer, M., Yang, L., Baltensperger, U., Haddad, I. El, Slowik, J. G., Cao, J., Pr, S. H., and Dusek, U.: Brown Carbon in Primary and Aged Coal Combustion Emission, Environ. Sci. Technol., 55, 5701–5710, https://doi.org/10.1021/acs.est.0c08084, 2021.

Qin, Y. M., Tan, H. B., Li, Y. J., Li, Z. J., Schurman, M. I., Liu, L., and Wu, C.: Chemical characteristics of brown carbon in atmospheric particles at a suburban site near Guangzhou, China, Atmos. Chem. Phys., 18, 16409–16418, 2018.

Vidovic, K., Jurkovic, D. L., Sala, M., Ana, K., and Grgic, I.: Nighttime Aqueous-Phase Formation of Nitrocatechols in the Atmospheric Condensed Phase, Environ. Sci. Technol., 52, 9722–9730, https://doi.org/10.1021/acs.est.8b01161, 2018.

Wang, F., Lu, Z., Lin, G., Carmichael, G. R., and Gao, M.: Brown Carbon in East Asia: Seasonality, Sources, and Influences on Regional Climate and Air Quality, ACS Environ. Au, 5, 128–137, https://doi.org/10.1021/acsenvironau.4c00080, 2024.

Wang, M., Duan, Y., Zhang, Z., Huo, J., Huang, Y., Fu, Q., Wang, T., Cao, J., and Lee, S.: Increased contribution to PM2.5 from traffic-influenced road dust in Shanghai over recent years and predictable future, Environ. Pollut., 313, 120119, https://doi.org/10.1016/j.envpol.2022.120119, 2022.

Wang, Q. and Yu, J. Z.: Ambient Measurements of Heterogeneous Ozone Oxidation Rates of Oleic, Elaidic, and Linoleic Acid Using a Relative Rate Constant Approach in an Urban Environment, Geophys. Res. Lett., 48, e2021GL095130, https://doi.org/10.1029/2021GL095130, 2021.

Wang, Q., He, X., Huang, X. H. H., Gri, S. M., Feng, Y., Zhang, T., Zhang, Q., Wu, D., and Yu, J. Z.: Impact of Secondary Organic Aerosol Tracers on Tracer-Based Source Apportionment of Organic Carbon and PM 2.5: A Case Study in the Pearl River Delta, China, ACS Earth Sp. Chem., 1, 562−571, https://doi.org/10.1021/acsearthspacechem.7b00088, 2017.

Wang, Q., Qiao, L., Zhou, M., Zhu, S., Griffith, S., Li, L., and Yu, J. Z.: Source Apportionment of PM 2.5 Using Hourly Measurements of Elemental Tracers and Major Constituents in an Urban Environment: Investigation of Time-Resolution Influence, J. Geophys. Res. Atmos., 123, 5284–5300, https://doi.org/10.1029/2017JD027877, 2018.

Wang, Q., Han, Y., Ye, J., Liu, S., and Pongpiachan, S.: High Contribution of Secondary Brown Carbon to Aerosol Light Absorption in the Southeastern Margin of Tibetan Plateau, Geophys. Res. Lett., 46, 4962–4970, https://doi.org/10.1029/2019GL082731, 2019a.

Wang, Q., Huang, X. H. H., Tam, F. C. V, Zhang, X., Man, K., Yeung, C., Feng, Y., Ying, Y., Ka, Y., Man, W., and Wu, C.: Source apportionment of fi ne particulate matter in Macao, China with and without organic tracers: A comparative study using positive matrix factorization, Atmos. Environ., 198, 183–193, https://doi.org/10.1016/j.atmosenv.2018.10.057, 2019b.

Wang, Q., Li, Z., Huang, Z., Zhu, S., Li, J., Qiao, L., Zhou, M., Huang, D., Wang, H., Fu, Q., Yu, H., and Yu, J. Z.: Day-by-day ambient determination of nighttime heterogeneous oxidation of particle-phase benzo[a]pyrene in an urban environment, Environ. Sci. Technol., 60, 11621–11630, 2026.

https://doi.org/10.5194/egusphere-2026-4766
Preprint. Discussion started: 18 August 2026

Wang, X., Heald, C. L., Sedlacek, A. J., Sá, S. S. De, Martin, S. T., Alexander, M. L., Watson, T. B., Aiken, A. C., Springston, S. R., and Artaxo, P.: Deriving brown carbon from multiwavelength absorption measurements: method and application to AERONET and Aethalometer observations, Atmos. Chem. Phys., 16, 12733–12752, https://doi.org/10.5194/acp-16-12733-2016, 2016.

Weingartner, E., Saatho, H., Schnaiter, M., and Streit, N.: Absorption of light by soot particles: determination of the absorption coe cient by means of aethalometers, J. Aerosol Sci., 34, 1445–1463, https://doi.org/10.1016/S0021-8502(03)00359-8, 2003.

Wu, C., Wu, D., and Yu, J. Z.: Quantifying black carbon light absorption enhancement with a novel statistical approach, Atmos. Chem. Phys., 18, 289–309, 2018.

Wu, L., Wu, C., Deng, T., Wu, D., Li, M., Li, Y. J., and Zhou, Z.: Field comparison of dual- and single-spot Aethalometers equivalent black carbon, light absorption, Ångström exponent, Atmos. Meas. Tech., 17, 2917–2936, 2024a.

Wu, Y., Liu, Q., Liu, D., Tian, P., Xu, W., Wang, J., Hu, K., Li, S., Jiang, X., Wang, F., Huang, M., Ding, D., Yu, C., and Hu, D.: Enhanced formation of nitrogenous organic aerosols and brown carbon after aging in the planetary boundary layer, npj Clim. Atmos. Sci., 7, 1–9, https://doi.org/10.1038/s41612-024-00726-x, 2024b.

Xiao, B., Wang, G., Li, Z., Li, R., Liang, C., Wang, H., Zhang, S., Wu, C., Li, R., Zhang, F., Zhang, R., Wu, Y., and Zhang, L.: High Contribution of Secondary Formation to Brown Carbon in China Humid Haze : Enhancing Role of Ammonia and Amines, Environ. Sci. Technol., 59, 27530–27540, https://doi.org/10.1021/acs.est.5c13436, 2025.

Xu, J., Priyadarshani, A., Hettiyadura, S., Liu, Y., Zhang, X., Kang, S., and Laskin, A.: Atmospheric Brown Carbon on the Tibetan Plateau: Regional Differences in Chemical Composition and Light Absorption Properties, Environ. Sci. Technol. Lett., 9, 219–225, https://doi.org/10.1021/acs.estlett.2c00016, 2022.

Yu, K., Zhu, Q., Du, K., and Huang, X.: Characterization of nighttime formation of particulate organic nitrates based on high-resolution aerosol mass spectrometry in an urban atmosphere in China, Atmos. Chem. Phys., 19, 5235–5249, 2019.

Yu, X., Zhou, M., Zhu, S., Qiao, L., Li, J., Ma, Y., and Zhang, Z.: Significant secondary formation of nitrogenous organic aerosols in an urban atmosphere revealed by bihourly measurements of bulk organic nitrogen and comprehensive molecular markers, Atmos. Chem. Phys., 25, 9061–9074, 2025.

Zhou, M., Nie, W., Qiao, L., Huang, D. D., and Zhu, S.: Elevated Formation of Particulate Nitrate From N2O5 Hydrolysis in the Yangtze River Delta Region From 2011 to 2019, Geophys. Res. Lett., 49, e2021GL097393, https://doi.org/10.1029/2021GL097393, 2022.

Zhu, S., Wang, Q., Qiao, L., Zhou, M., Wang, S., Lou, S., Huang, D., Wang, Q., Jing, S., Wang, H., and Chen, C.: Tracer-based characterization of source variations of PM2.5 and organic carbon in Shanghai in fluenced by the COVID-19 lockdown, Faraday Discuss., 226, 112–137, https://doi.org/10.1039/D0FD00091D, 2021.

Zhu, S., Zhang, J., Li, L., Zhou, M., Qiao, L., Wang, H., Huang, D., Wang, Q., Jing, S., Wu, Y., Wang, S., Chen, C., Ying, Q., and Yu, J. Z.: Aerosol uptake coefficients of isoprene epoxides: determination and parameter estimation from online field measurements of organic molecular markers, Environ. Sci. Technol., 59, 18249–18258, 2025.